Methane Activation

DOI: 10.1002/anie.200((will be filled in by the editorial staff))

Vacuum Ultraviolet Photoionization Studies of $PtCH_2$ and H-Pt-CH_3: A Potential Energy Surface for the Pt + CH_4 Reaction

Manori Perera, Ricardo B. Metz, Oleg Kostko and Musahid Ahmed*

Activation of methane is a long-standing goal of catalysis, due to its potential industrial utility as an inexpensive hydrocarbon feedstock, and is of interest as the most fundamental C-H bond activation reaction.[1] The observation that several gas-phase third-row transition metal cations M^+ efficiently dehydrogenate methane at room temperature[2]

$$M^+ + CH_4 \rightarrow MCH_2^+ + H_2$$

has led to extensive gas-phase studies of reactions of metal atoms, ions and clusters with methane.[See [1-3] and references therein] These studies provide valuable information regarding reaction mechanisms, the energetics and structures of intermediates and of critical barriers. These results inform the choice of metal, cluster size, support and ligand properties in a potential catalyst. In addition, they serve as a benchmark against which the accuracy of computational studies can be assessed. Due to its importance as an industrial catalyst, reactions of Pt and Pt^+ with methane have received particular attention. At thermal energies, Pt^+ reacts at ~50% of the collision rate, producing $PtCH_2^+$.[2, 3c, 4] Guided ion beam (GIB) experiments have measured the overall exothermicity of the reaction, as well as the stability of the $[H\text{-}Pt\text{-}CH_3]^+$ insertion intermediate.[5] Neutral metal atoms are much less reactive than the cations. This has been attributed to the absence of long-range ion-induced dipole attraction, and the lack of low-lying reactive (low-spin d^n or $d^{n-1}s$) electronic states. Carroll et al. find that platinum is unique in activating methane at thermal energies.[6] Campbell confirms the reactivity of Pt, at ~3% of the collision rate.[7] These kinetics studies monitor Pt via laser-induced fluorescence, but do not observe products. As a result, it is difficult to determine to what extent loss of Pt is due to true bimolecular reaction, producing $PtCH_2 + H_2$, and to what extent it is due to termolecular formation of the H-Pt-CH_3 insertion intermediate, which is stabilized by collisions with the buffer gas. These kinetics studies do not determine the reaction mechanism or provide much information on the potential energy surface. A number of questions remain outstanding. How endothermic is dehydrogenation of methane by atomic platinum? How stable is the insertion intermediate, and is there a barrier to its formation? This study addresses these questions, determining the energetics of H-Pt-CH_3 and $PtCH_2$ by coupling photoionization measurements of their ionization energy with guided ion beam (GIB) measurements of the thermodynamics of the corresponding cations.[5] In addition, spin-orbit DFT (SODFT) calculations are used to characterize other intermediates and the barriers that separate them. Comparison of the potential energy surfaces for the reactions of Pt and Pt^+ with CH_4 shows that charge has surprisingly little effect on the potential energy surface for this most fundamental C-H activation reaction.

The laser ablation experiments are performed using tunable VUV light accessed at a synchrotron (Advanced Light Source (ALS) at Lawrence Berkeley National Laboratory). The molecules of interest are produced using a pulsed laser ablation source[8] and ionized using tunable VUV light. The resulting ions are extracted into a reflectron time-of-flight mass spectrometer and tallied using a fast counter. Photoionization efficiency curves (PIE) are measured by integrating the area under the photo-ion of interest and normalizing to ALS current and VUV flux. Further details are available in the Supporting Information.

Figure 1 shows the PIE of $PtCH_2$ and H-Pt-CH_3 near the ionization onset. The figures also show simulated PIE spectra. They are calculated by computing the geometries and vibrations of the neutral and cation, and calculating Franck-Condon factors for each vibration. The products of the Franck-Condon factors are then integrated and convolved with the 25 meV VUV Gaussian linewidth to generate the PIE spectrum.[9] The electronic structure calculations are described in more detail below. For these two molecules, there is little geometry change upon ionization, leading to a sharp onset in the PIE. The ionization energy is determined by shifting the energy origin of the simulation until it provides the best match to the PIE spectrum. This procedure determines the ionization energy of $PtCH_2$ to be 8.78±0.03 eV. The IE(H-Pt-CH_3) is slightly higher: 8.89±0.03 eV. These values are very slightly lower than IE(Pt)=8.959 eV.

The PIE spectrum clearly shows that the $[Pt,C,H_4]^+$ ion is formed by photoionization of the H-Pt-CH_3 insertion intermediate and is not due to a Pt(CH_4) entrance channel van der Waals complex. First, in an entrance channel complex, CH_4 would interact much more strongly with Pt^+ than it does with neutral Pt, due to the strong ion-induced dipole force. This would lead to an ionization energy of Pt(CH_4) at least 0.5 eV lower than that of Pt. In addition, the large change in geometry between the neutral and cation entrance channel complexes would lead to a very gradual onset in the PIE. Furthermore, the calculations predict that there is no barrier to Pt

[*] Prof. R.B. Metz

Dept. of Chemistry
University of Massachusetts Amherst
Amherst, MA 01003 USA
E-mail: rbmetz@chem.umass.edu

Prof. M. Perera
Dept. of Chemistry
Illinois Wesleyan University
Bloomington, IL 61702 USA

Dr. O. Kostko, Dr. M. Ahmed
Chemical Sciences Division
Lawrence Berkeley National Laboratory
Berkeley, CA 94720 USA

[**] MA and OK gratefully acknowledge support from the Director, Office of Energy Research, Office of Basic Energy Sciences, Chemical Sciences Division of the U.S. Department of Energy under contract No. DE-AC02-05CH11231. MP and RBM gratefully acknowledge the support of the National Science Foundation under Award CHE-0911225.

Supporting information for this article is available on the WWW under http://www.angewandte.org.

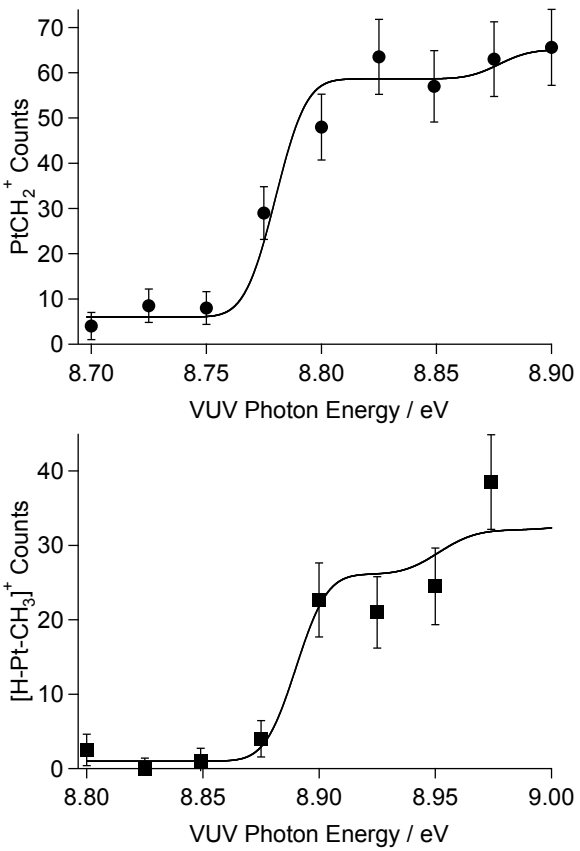

Figure 1. Photoionization efficiency spectra for $PtCH_2$ (upper) and H-Pt-CH_3 (lower) and simulations. The VUV line width is 25 meV. Each point includes data from 10000 ablation laser pulses.

insertion into the C-H bond in methane, so there is no stable entrance channel complex.

Bond dissociation energies for neutral, platinum-containing molecules are calculated by combining our ionization energies with the bond dissociation energies measured in the GIB experiments of Zhang et al.[5] for the corresponding cations. All thermodynamic values are at 0 K. The bond dissociation energy of $PtCH_2$ is

$$D_0(Pt\text{-}CH_2) = D_0(Pt^+\text{-}CH_2) + IE(PtCH_2) - IE(Pt) \qquad (1)$$

Zhang et al. determined $D_0(Pt^+\text{-}CH_2)$= 4.80±0.03 eV.[5] In conjunction with the measured $IE(PtCH_2)$= 8.78 ± 0.03 eV, this gives $D_0(Pt\text{-}CH_2)$=4.62 ± 0.04 eV (446 ± 4 kJ mol^{-1}).

This can then be used to calculate the energetics of dehydrogenation of methane by the platinum atom. Formation of $CH_2 + H_2$ from CH_4 is endoergic by 454.7 ± 2.5 kJ mol^{-1}.[5] Thus, the bimolecular Pt + CH_4 → $PtCH_2$ + H_2 reaction is endoergic, but only by 9 ± 5 kJ/mol. A second key finding in our work is the energy of the H-Pt-CH_3 insertion intermediate. GIB studies of collisions of $[H\text{-}Pt\text{-}CH_3]^+$ with Xe determine that it lies 1.77±0.08 eV below Pt^+ + CH_4.[5] Combining this result with IE(H-Pt-CH_3)=8.89±0.03 eV means that insertion of neutral Pt into CH_4 to form H-Pt-CH_3 is exoergic by 1.70 ± 0.09 eV (164±9 kJ/mol).

Is there a barrier to insertion of platinum into the C-H bond in methane? The B3LYP calculations of Xiao and Wang predict that there is a 116 kJ mol^{-1} barrier for the ^3D (d^9s) ground state of Pt to insert into methane, while insertion is barrierless for the ^1S (d^{10}) excited state.[10] Although they did not calculate the energy of the singlet-triplet crossing, an earlier calculation predicts it to occur at an energy of 5 kJ mol^{-1}.[6] Second order spin-orbit coupling causes these two states to interact and repel. We carried out electronic structure calculations which include this effect using spin-orbit density functional theory (SODFT)[11] in the *NWChem*[12] electronic

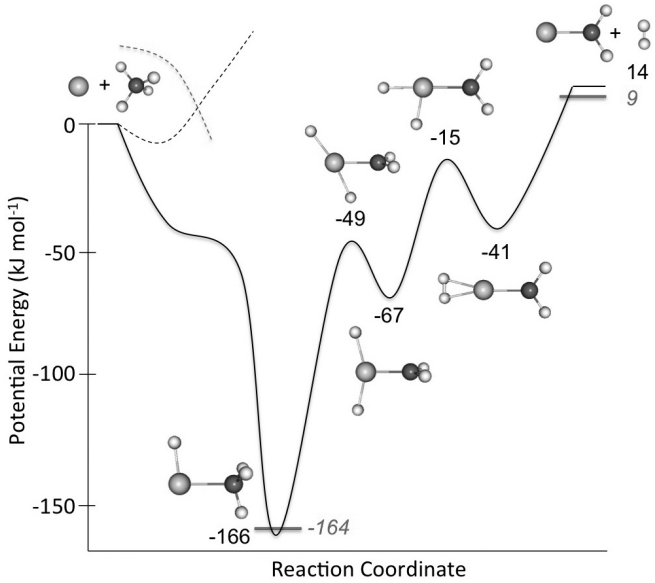

Figure 2. Potential energy surface for the Pt + CH_4 reaction. The solid curve and corresponding structures of intermediates and transition states are calculated using spin-orbit DFT with the B3LYP functional and aug-cc-pVTZ basis set. The lower and upper dashed lines are the result of conventional B3LYP calculations for the ground triplet state and lowest singlet state. Horizontal lines and values in italics indicate experimentally determined energies.

structure package. Structures and vibrational frequencies of intermediates and transition states are in Supporting Information.

Figure 2 shows a potential energy surface for the Pt + CH_4 reaction calculated using SODFT. Also, the dashed lines show the result of conventional B3LYP calculations, without spin-orbit coupling. Approach of the ground (^3D, d^9s^1) state of Pt to methane leads to a weakly bound entrance channel complex. C-H bond insertion by triplet Pt involves a substantial barrier, agreeing with previous calculations.[6, 10] In contrast, insertion of the lowest singlet state (^1S, d^{10}) of Pt into the C-H bond is barrierless. After the triplet-singlet crossing, the minimum energy path for the reaction occurs exclusively on the singlet surface. The SODFT calculations show that the spin-orbit interaction between the triplet and singlet pathways in the entrance channel is so strong that there is no barrier to insertion of platinum into the C-H bond. Despite a careful search, no transition state for this insertion could be located. On the minimum energy path, there is no local minimum corresponding to the Pt(CH_4) entrance channel complex. The insertion intermediate is calculated to lie 166 kJ mol^{-1} below reactants. This is in excellent agreement with the experimental value of 164±9 kJ mol^{-1}. As proposed by Xiao and Wang,[10] on the minimum energy path the reaction proceeds by sequential H-transfer to produce dihydrido H,H-$PtCH_2$ and (H_2)$PtCH_2$, which then dissociates to form $PtCH_2$ ($^1A_1$) + H_2. Recently, vibrational spectra of H-Pt-CH_3 and, perhaps, H,H-$PtCH_2$ have been measured in a cryogenic Ar matrix.[13] The SODFT calculations predict that the overall reaction is 14 kJ mol^{-1} endoergic, again in excellent agreement with the experimental result, 9±5 kJ mol^{-1}. Our calculations predict that the barriers all lie well below the $PtCH_2$ + H_2 products.

A comparison of the SODFT results with conventional B3LYP calculations with the same basis set gives very similar results for the relative energies of H-Pt-CH_3, the later intermediates, and the products (all of which are singlets). The two calculations differ significantly, however, in the energies of the reactants and entrance channel complex. This agrees with the assertion by Carroll et al.[6] that spin-orbit effects are most significant for the bare atom and non-covalent complexes and that they are largely quenched by

formation of covalent bonds. In addition, the previous calculations[6, 10, 14] predicted intermediates, transition states and products that are at least 20 kJ mol^{-1} less stable relative to reactants than our calculations. This is primarily due to our use of the larger, more flexible aug-cc-pVTZ-PP basis set for Pt[15] and, to a lesser extent, to including spin-orbit effects.

The kinetics of the reactions of neutral and cationic platinum atoms with methane are quite different. At 300 K, reaction of the neutral is quite inefficient, with an observed bimolecular rate that corresponds to 3% of the collision rate. This has been interpreted as being due to formation and efficient termolecular stabilization of the H-Pt-CH_3 intermediate, with negligible formation of bimolecular products $PtCH_2$ + H_2. This view was partly due to calculations done in conjunction with the kinetics study which predicted that conversion of H-Pt-CH_3 to the $(H_2)PtCH_2$ exit channel complex involves a 129 kJ mol^{-1} barrier, as it occurs *via* a concerted pathway involving a four-center intermediate.[6] The kinetics results were thus interpreted as being solely due to the termolecular pathway, operating near the high pressure limit. In contrast, the Pt^+ cation, under single-collision conditions and at 300 K, reacts with CH_4 at 80% of the collision rate, forming $PtCH_2^+$ + H_2.[4c] In the presence of buffer gas, the insertion intermediate is also observed.[5] The kinetics studies[6] concluded that charge matters: the attractive ion-induced dipole interaction stabilizes all adducts relative to reactants. This lowers the energies of intermediates and reduces barriers, facilitating the reaction. Our study turns the aforementioned conclusion on its head. For activation of methane by platinum, charge matters very little! The mechanisms and energetics of the reactions of Pt and Pt^+ [5] with methane are very similar. In both cases insertion of the metal into the C-H bond is barrierless, and leads to insertion intermediates with high, and very similar, stabilities. Subsequent hydrogen transfer from the methyl group to the metal is sequential, with calculated barriers which lie below the energy of the dehydrogenation products. The major difference in the observed kinetics is likely due to the 18 kJ mol^{-1} difference between the Pt^+-CH_2 and Pt-CH_2 bond strength. As a result, dehydrogenation of methane by Pt^+ is slightly exoergic, while reaction with neutral Pt is slightly endoergic.

The energetics of two key species involved in methane activation by platinum atom - the H-Pt-CH_3 insertion intermediate and $PtCH_2$ + H_2 products - have been determined by combining measured ionization energies with bond dissociation energies for the corresponding cations obtained in guided ion beam experiments. Coupled with kinetics experiments and high-level electronic structure calculations, these findings provide unprecedented insight into the mechanistic details of this most fundamental C-H bond activation reaction.

Received: ((will be filled in by the editorial staff))
Published online on ((will be filled in by the editorial staff))

Keywords: C-H bond activation · methane activation · reaction intermediates · platinum · photoionization

[1] H. Schwarz, *Angew. Chem. Intl. Ed.* **2011**, *50*, 10096-10115.
[2] K. K. Irikura, J. L. Beauchamp, *J. Phys. Chem.* **1991**, *95*, 8344-8351.
[3] a) P. B. Armentrout, *Annu. Rev. Phys. Chem.* **2001**, *52*, 423-461; b) D. K. Böhme, H. Schwarz, *Angew. Chem. Int. Ed.* **2005**, *44*, 2336-2354; c) A. Shayesteh, V. V. Lavrov, G. K. Koyanagi, D. K. Bohme, *J. Phys. Chem. A* **2009**, *113*, 5602-5611; d) J. Roithova, D. Schröder, *Chem. Rev.* **2010**, *110*, 1170-1211.
[4] a) C. Heinemann, R. Wesendrup, H. Schwarz, *Chem. Phys. Lett.* **1995**, *239*, 75-83; b) K. Koszinowski, D. Schröder, H. Schwarz, *J. Phys. Chem. A* **2003**, *107*, 4999-5006; c) M. Pavlov, M. R. A. Blomberg, P. E. M. Siegbahn, R. Wesendrup, C. Heinemann, H. Schwarz, *J. Phys. Chem. A* **1997**, *101*, 1567-1579.
[5] X. G. Zhang, R. Liyanage, P. B. Armentrout, *J. Am. Chem. Soc.* **2001**, *123*, 5563-5575.
[6] J. J. Carroll, J. C. Weisshaar, P. E. M. Siegbahn, C. A. M. Wittborn, M. R. A. Blomberg, *J. Phys. Chem.* **1995**, *99*, 14388-14396.
[7] M. L. Campbell, *J. Chem. Soc. Faraday Trans.* **1998**, *94*, 353-358.
[8] a) C. Nicolas, J. Shu, D. S. Peterka, L. Poisson, S. R. Leone, M. Ahmed, *J. Am. Chem. Soc.* **2006**, *128*, 220-226; b) M. Citir, R. B. Metz, L. Belau, M. Ahmed, *J. Phys. Chem. A* **2008**, *112*, 9584-9590; cS. R. Leone, M. Ahmed, K. R. Wilson, *Phys. Chem. Chem. Phys.* **2010**, *12*, 6564-6578.
[9] C. A. Taatjes, D. L. Osborn, T. A. Cool, K. Nakajima, *Chem. Phys. Lett.* **2004**, *394*, 19-24.
[10] L. Xiao, L. C. Wang, *J. Phys. Chem. B* **2007**, *111*, 1657-1663.
[11] P. Nichols, N. Govind, E. J. Bylaska, W. A. de Jong, *J. Chem. Th. Comput.* **2009**, *5*, 491–499.
[12] M. Valiev, E. J. Bylaska, N. Govind, K. Kowalski, T. P. Straatsma, H. J. J. van Dam, D. Wang, J. Nieplocha, E. Apra, T. L. Windus, W. A. de Jong, *Comput. Phys. Commun.* **2010**, *181*, 1477-1489.
[13] H.-G. Cho, L. Andrews, *J. Phys. Chem. A* **2008**, *112*, 12293-12295.
[14] Q. Cui, D. G. Musaev, K. Morokuma, *J. Chem. Phys.* **1998**, *108*, 8418-8428.
[15] D. Figgen, K. A. Peterson, M. Dolg, H. Stoll, *J. Chem. Phys.* **2009**, *130*, 164108-164112.

Entry for the Table of Contents (Please choose one layout)

Layout 1:

Methane Activation

Prof. Manori Perera, Prof. Ricardo B. Metz,* Dr. Oleg Kostko, Dr. Musahid Ahmed _____ **Page – Page**

Vacuum Ultraviolet Photoionization Studies of $PtCH_2$ and H-Pt-CH_3: A Potential Energy Surface for the Pt + CH_4 Reaction

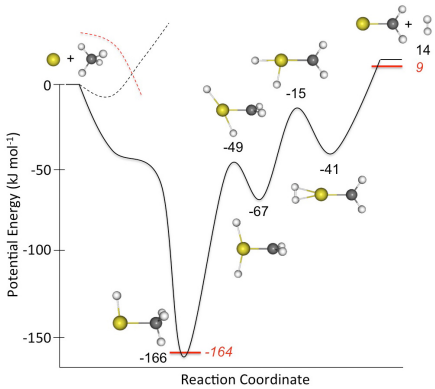

Does Charge Matter? Direct VUV measurement of ionization energies reveals that C-H insertion by Pt to form H-Pt-CH_3 is highly exoergic, while production of $PtCH_2$ + H_2 is slightly endoergic. Experiments and SODFT calculations reveal surprisingly similar energetics.for dehydrogenation of methane by neutral and cationic platinum.

Layout 2:

((Catch Phrase))

((Author(s), Corresponding Author(s)*))
_____ **Page – Page**

((Title Text))

((TOC Graphic))

((Text for Table of Contents, max. 450 characters))

Supporting Information

Vacuum Ultraviolet Photoionization Studies of $PtCH_2$ and H-Pt-CH_3:
A Potential Energy Surface for the Pt + CH_4 Reaction

Manori Perera, Ricardo B. Metz, Oleg Kostko and Musahid Ahmed*

Experimental Details

Laser ablation of a platinum tube produces platinum atoms that then react with methane gas from a pulsed piezoelectric valve at 200 kPa backing pressure. The Nd:YAG ablation laser operates at a repetition rate of 50 Hz and can produce up to 8 mJ/pulse at 532 nm. High laser power favors production of PtC, observed in our previous study,[1] while production of $PtCH_2$ and H-Pt-CH_3 is optimum at 3 mJ/pulse. The molecules cool in the supersonic expansion. The molecular beam is skimmed and the neutral molecules are irradiated by VUV light. The beamline provides vacuum ultraviolet (VUV) light with photon energies of 8-16 eV at a repetition rate of 500 MHz. The spectral line width is determined by the slit width on a 3 m monochrometer. A pulsed voltage extracts neutrals that are ionized by the VUV light into a time-of-flight reflectron mass spectrometer. Masses of photoions are determined by their flight times to a dual micro channel plate detector.

Mass spectra are obtained as a function of VUV photon energy, typically summing over 5000-10000 laser shots at each energy. Photoionization efficiency curves (PIE) are measured by integrating the area under the photo-ion of interest and normalizing to ALS current and VUV flux as measured by a Si photodiode. Survey scans with 1500 μm slit width (~50 meV line width at 9 eV) are used to identify the products and estimate the onset region for each. Fine scans, with 800 μm slits (~25 meV at 9 eV), near each onset are used to determine ionization energies.

Platinum has four major isotopes: ^{194}Pt (33%), ^{195}Pt (34%), ^{196}Pt (25%), and ^{198}Pt (7%). To avoid isobaric interferences, initial studies to identify the reaction products used deuterated methane. Figure S1 shows a mass spectrum obtained by ablating platinum in CD_4. As platinum-195 is the only odd mass isotope, products with odd mass must contain ^{195}Pt. Only the "even deuterium" species with stoichiometry PtC, $PtCD_2$ and $PtCD_4$ are observed, along with a small amount of PtC_2D_n. Under these conditions, PtCD and $PtCD_3$ are not formed. So, subsequent experiments employed CH_4, and the ^{195}Pt-containing peak

was typically monitored, as it is uniquely present in all odd mass peaks (see Fig. S2 for a mass spectrum).

It is important to find a peak that is not contaminated by isobaric interferences. For the insertion intermediate this is accomplished by monitoring only H-^{195}Pt-CH_3 at m/z = 211 amu. The results shown for the carbene include data from $^{194}PtCH_2$ and $^{195}PtCH_2$. The $^{194}PtCH_2$ data is included because ^{196}PtC does not contribute in this energy region as the IE(PtC)=9.45±0.05 eV.[1]

Electronic structure calculations were carried out with the *NWChem*[2] electronic structure package using spin-orbit density functional theory (SODFT)[3] with the B3LYP hybrid density functional. SODFT is a two-component approximation to the relativistic Dirac equations, which, when used in conjunction with relativistic effective core potentials, accurately reproduces properties which depend on the valence electrons, such as geometries and bond strengths, with far less computational effort than a full, all-electron relativistic calculation.[3-4] The aug-cc-pVTZ-PP relativistic effective core potential, basis set and spin-orbit parameters[5] was used for platinum. The aug-cc-pVTZ basis set was used for carbon and hydrogen. Harmonic frequencies were calculated at each stationary point to ensure that it is a minimum or transition state. All reported energies include the zero-point contribution, using unscaled harmonic frequencies. Basis set superposition error (BSSE) was estimated for $(H_2)PtCH_2$ using the counterpoise method. It amounted to <1 kJ/mol, and thus was not included in the reported results.

Initial calculations used the SDD basis and effective core potential for Pt. To improve the flexibility of the basis set, additional valence and polarization functions were added. This addition consistently increased the stability of the intermediates and products relative to reactants. Thus, for example, insertion of Pt into methane is calculated to be exoergic by 130 kJ/mol using the SDD basis and by 144 kJ/mol with an SDD basis augmented with valence functions (s: exponent=0.03, 0.3; p: 0.045, 0.2; d: 0.025, 0.09, 0.3) and polarization functions (f: 0.443, 1.323; g: 1.1). Use of the larger aug-cc-pVTZ-PP basis and effective core potential results in a further increase, to 166 kJ/mol.

References

[1] M. Citir, R. B. Metz, L. Belau, M. Ahmed, *J. Phys. Chem. A* **2008**, *112*, 9584-9590.

[2] M. Valiev, E. J. Bylaska, N. Govind, K. Kowalski, T. P. Straatsma, H. J. J. van Dam, D. Wang, J. Nieplocha, E. Apra, T. L. Windus, W. A. de Jong, *Comput. Phys. Commun.* **2010**, *181*, 1477-1489.

[3] P. Nichols, N. Govind, E. J. Bylaska, W. A. de Jong, *J. Chem. Th. Comput.* **2009**, *5*, 491–499.

[4] F. Rakowitz, C. M. Marian, B. Schimmelpfennig, *Phys. Chem. Chem. Phys.* **2000**, *2*, 2481-2488.

[5] a) D. Andrae, U. Häussermann, M. Dolg, H. Stoll, H. Preuss, *Theor. Chim. Acta* **1990**, *77*, 123-141; b) D. Figgen, K. A. Peterson, M. Dolg, H. Stoll, *J. Chem. Phys.* **2009**, *130*, 164108-164112.

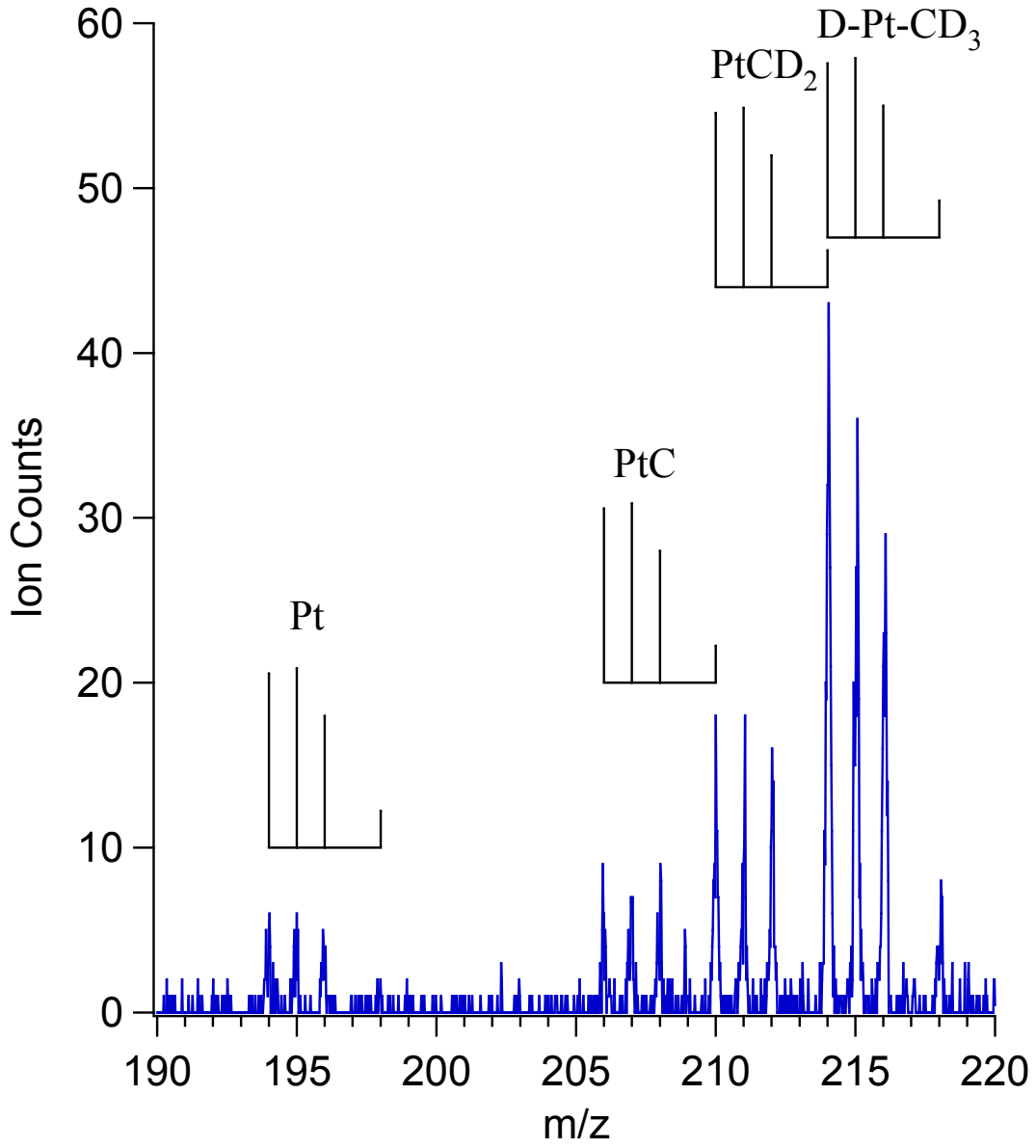

Figure S1. The mass spectrum of the ionized products from the reaction of laser-ablated platinum with CD_4 at 11 eV. The combs show the assignment of the $PtCD_n$ peaks, with the relative abundances of the platinum isotopomers.

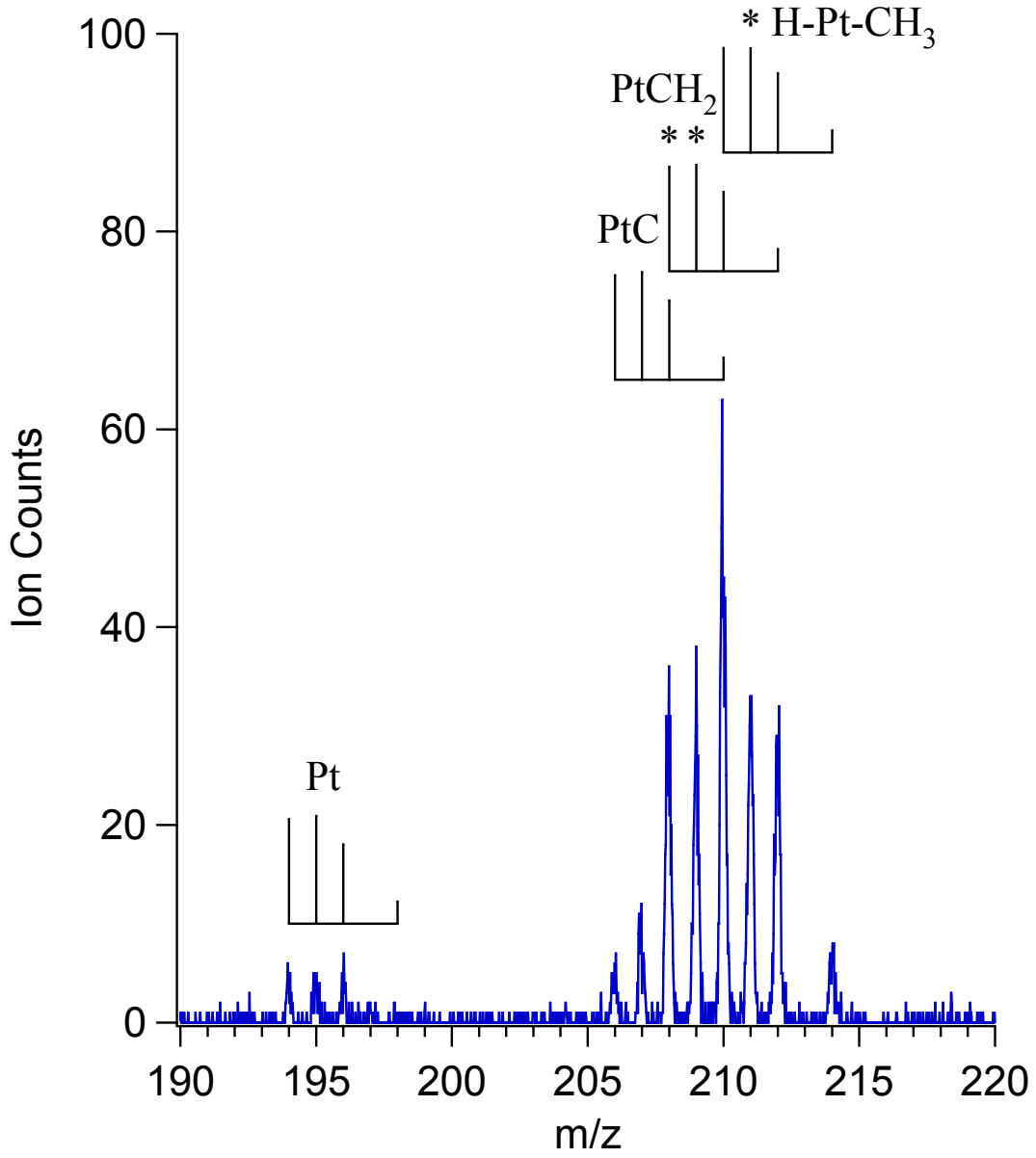

Figure S2. The mass spectrum of the ionized products from the reaction of laser-ablated platinum with CH_4 at 11 eV. The combs show the assignment of the $PtCH_n$ peaks, with the relative abundances of the platinum isotopes. $PtCH_2$ can be monitored without isobaric interferences at m/z=209; it can also be detected at m/z=208 below IE(PtC)=9.45 eV. $HPtCH_3$ can be monitored without isobaric interferences at m/z=211. These masses are denoted with asterisks.

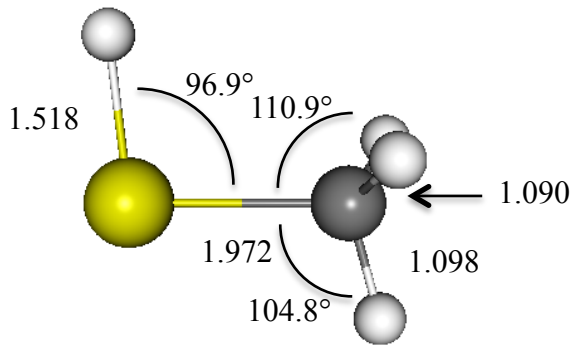

H-Pt-CH_3

A=3.067, B=0.280, C=0.270
121 torsion
469 C-Pt-H bend
619 Pt-C stretch
785 *(800.6)* asym. CH_3 rock
818 *(838.4)* sym. CH_3 rock
1215 *(1266.2)* CH_3 deformation
1419 CH_3 asym. bend
1434 CH_3 sym. bend
2360 *(2416.4)* Pt-H stretch
3035 *(2977.2)* sym. C-H stretch
3116 *(3078.2)* sym. C-H stretch
3135 asym. C-H stretch
Wavenumbers measured in Ar matrix (H.-G. Cho, L. Andrews, *J. Phys. Chem. A* **2008,** *112,* 12293-12295) are in italics.

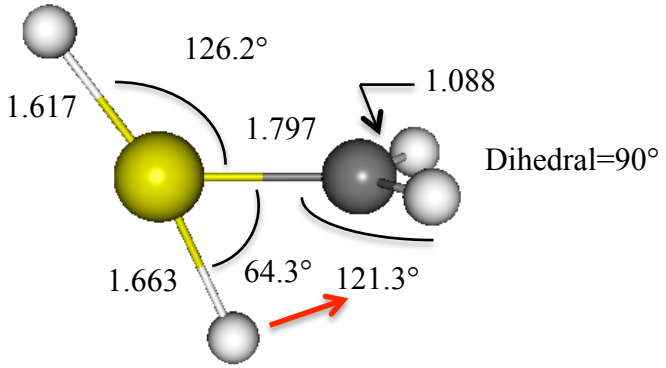

TS2

A=3.001, B=0.337, C=0.329
700 *i* shown with red arrow
403, 659, 693, 859, 878,1065, 1406, 1944, 2160, 3062, 3169

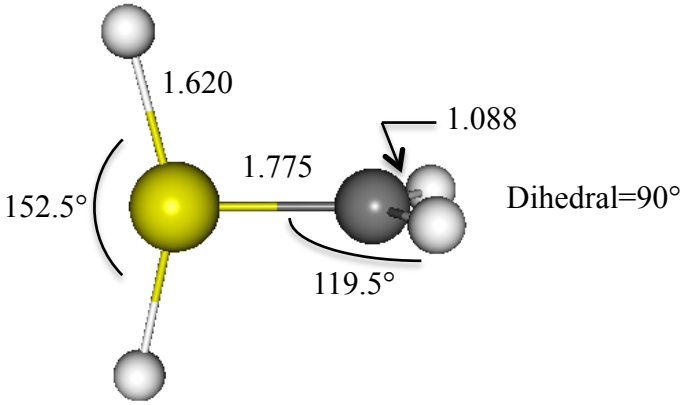

H,H-PtCH_2

A=2.480, B=0.354, C=0.331
(note: in-plane is in plane of paper)
282 in-plane PtH_2 wag
456 out-of-plane PtH_2 wag
599 torsion
767 H-Pt-H bend
847 out-of-plane CH_2 wag
884 Pt-C stretch
937 in-plane CH_2 wag
1392 H-C-H bend
1967 asym. Pt-H stretch*
2144 sym. Pt-H stretch
3062 asym. C-H stretch
3191 asym. C-H stretch

*tentatively observed at 1901.6 cm^{-1} in an Ar matrix. (H.-G. Cho, L. Andrews, *J. Phys. Chem. A* **2008,** *112,* 12293-12295)

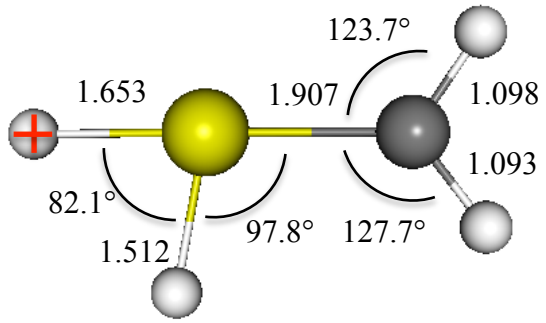

TS3

A=4.394, B=0.299, C=0.280
431 *i* Shown in red (out of plane)
350, 379, 510, 683, 831, 1090,
1430, 2004, 2433, 3004, 3084

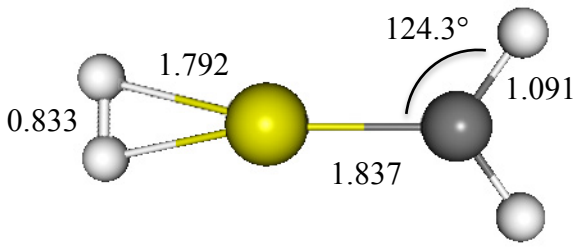

$(H_2)PtCH_2$

A=8.434, B=0.300, C=0.296
79 H_2 out-of-plane bend
309 H_2 in-plane wag
704 Pt-C stretch
735 H_2 out-of-plane twist
759 CH_2 in-plane wag
1006 Pt-H_2 stretch
1063 CH_2 out-of-plane wag
1407 H-C-H bend
1633 H-Pt-H asym. stretch
3055 C-H sym. stretch
3127 C-H asym. stretch
3135 H-H stretch

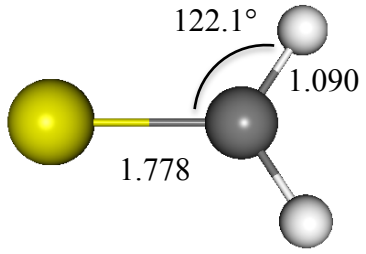

$PtCH_2$

A=9.812, B=0.367, C=0.354
832 in-plane CH_2 wag
843 Pt-C stretch
1066 out-of-plane bend
1415 H-C-H bend
3045 C-H sym. stretch
3140 C-H asym. stretch

Figure S3. Structures, rotational constants and vibrational frequencies of intermediates and transition states of the Pt + CH_4 reaction. Calculations using spin-orbit DFT, with the B3LYP hybrid density functional, and the aug-cc-pVTZ-PP basis set and effective core potential for Pt, and the aug-cc-pVTZ basis set for C and H. Frequencies are unscaled.

This document was prepared as an account of work sponsored by the United States Government. While this document is believed to contain correct information, neither the United States Government nor any agency thereof, nor the Regents of the University of California, nor any of their employees, makes any warranty, express or implied, or assumes any legal responsibility for the accuracy, completeness, or usefulness of any information, apparatus, product, or process disclosed, or represents that its use would not infringe privately owned rights. Reference herein to any specific commercial product, process, or service by its trade name, trademark, manufacturer, or otherwise, does not necessarily constitute or imply its endorsement, recommendation, or favoring by the United States Government or any agency thereof, or the Regents of the University of California. The views and opinions of authors expressed herein do not necessarily state or reflect those of the United States Government or any agency thereof or the Regents of the University of California.